DIURNAL AND SEASONAL VARIATIONS OF WATER VAPOUR AND CLOUD WATER ATTENUATION IN MICROWAVE FREQUENCY BANDS

Ondřej Fišer, Daniela Řezáčová
Dept. of Meteorology
Institute of Atmospheric Physics AS CR
Boční 2, 141 31 Prague 4
Czech Republic

Abstract

20 years of radiosonde data from the aerological station Prague-Libus were analysed to evaluate integrated values of water vapour content and cloud water content. Both parameters are proportional to the attenuation in microwave frequency bands. The soundings from 00, 06, 12, and 18 UTC were taken into account to discuss diurnal as well as seasonal variations. The methods available to compute the cloud and the water vapour attenuation are presented.

Keywords

Water vapour content (WVC), Cloud water content (CWC) , Diurnal and Seasonal variations, Atmospheric Attenuation, Radiowave propagation

1. Introduction

Many papers have dealt with the distribution of water vapour and/or cloud (liquid) water attenuation on microwave satellite paths (see, for example, [1], [2] and [3]). The distribution of zenith attenuation has been the usual output form; the path attenuation can be obtained by dividing the zenith attenuation value by the sine of the elevation angle (for elevations above 5°). At present the attention is paid to the description of the diurnal as well as the seasonal variations of the atmospheric attenuation. The first attempt to assess the variations from the Czech aerological data is discussed in this study.

2. Input Data

The present study is based on radiosonde data from the station Prague - Libus measured at 00, 06, 12, and 18 UTC during the period 1971-1991. Fig.1 shows the number of soundings in each month at corresponding time. It is obvious that we processed more than 400 series of vertical profiles for each of the times considered. Various population extends bear no significant influence on the results.

The input data contains the vertical profiles of height, temperature, pressure and relative humidity. The data was recorded at heights above the ground level of the aerological station (304 m above sea level).

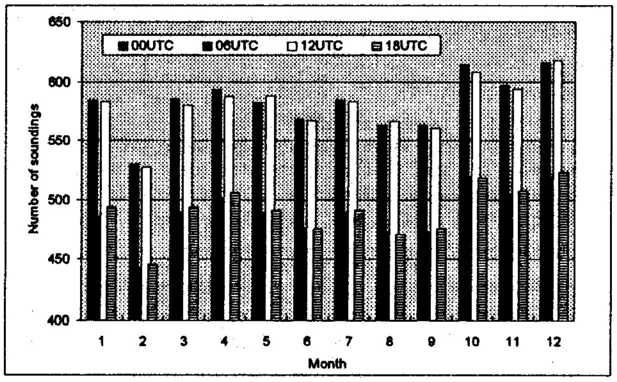

Fig.1: Absolute frequency of Prague-Libus soundings used in the study. The time period involves the years 1971-1991. Soundings corresponding to the 00UTC, 06UTC, 12UTC, and 18UTC are considered.

3. Microwave Attenuation through the Water Vapour

3.1. Exact Technique

We have chosen the method of Dr. Liebe which is often used to compute the specific water vapour attenuation γ while the input parameters are: water vapour partial pressure, dry air pressure, air temperature and frequency [4]. The total (zenith) water vapour attenuation [dB] is given by the integral:

$$A_v = \int_{h_s}^{h_u} \gamma(h)dh \qquad (1)$$

where h_s and h_u is the height above the sea level of the radiosonde base, and upper limit of the water vapour occurrence, respectively (in [3] it is supposed to stop the integration at the air pressure level of 300 hPa).

Combination of diurnal and month course of the attenuation on given exceedance probability levels is shown in Fig.2a (for 1% exceedance probability, frequency is a parameter) and in Fig.2b (for 20 GHz, exceedance probability is a parameter). The four values plotted for each average month (from left to right) correspond to the diurnal measurement at 00, 06,12 and 18 UTC (also in further figures).

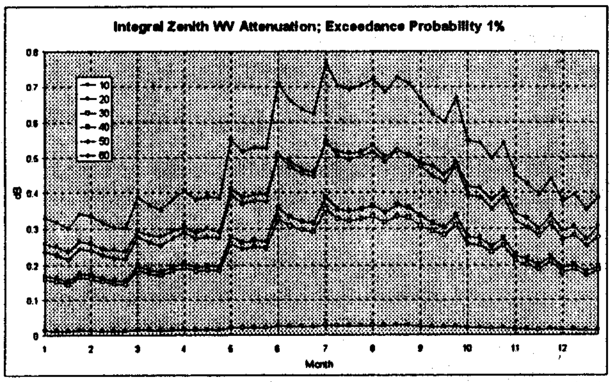

Fig.2a: Integral Zenith Water Vapour Attenuation [dB], which is exceeded at 1% of 6 hour periods considered. The frequency in [GHz] is shown in the legenda

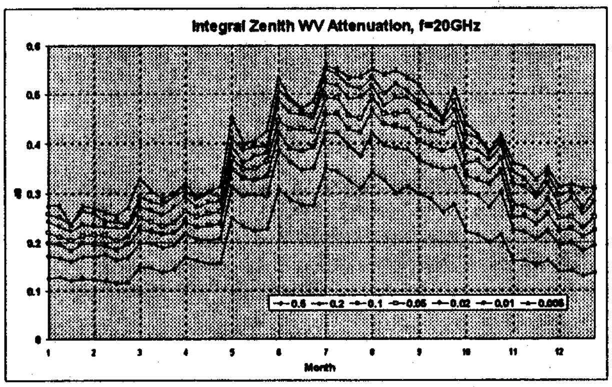

Fig.2b: Integral Zenith Water Vapour Attenuation [dB] at the frequency 20GHz, which is exceeded at X% of 6hour periods considered. Values of X are shown in the legenda.

3.2. Engineering Technique

The exact technique to compute the specific water vapour attenuation γ depends also on the frequency. To avoid this disadvantage the authors of [3] have proposed the following approximation to compute the total zenith water vapour attenuation, which is simply proportional to the integrated water vapour content *WVC*:

$$A = 0.0173\frac{\gamma\{f, p_{ref}, \rho_{ref}, t_{ref}\}}{\gamma\{f_{ref}, p_{ref}, \rho_{ref}, t_{ref}\}} * WVC \qquad (2)$$

where (in accordance with [3])
p_{ref}=780hPa, ρ_{ref}=WVC/4km, t_{ref}= 14ln(0.22ρ_{ref})+3°C, f_{ref}=20.6GHz, and *WVC* is the integrated water vapour content defined by equation (3).

Comparison of the results of the exact method with the simplified method in frequency range 10-60 GHz has shown a very good fit. Therefore the study of diurnal and seasonal variation of the water vapour attenuation can be reduced to the study of the *WVC* variation, only.

3.3. Diurnal and Seasonal Variations of the Integrated Water Vapour Content

The zenith integrated water vapour content [kg/m^2] is defined by the equation:

$$WVC = \int_{h_s}^{h_u} \rho(h)dh \qquad (3)$$

where ρ is the water vapour density [kg/m^3], h is the height [m], h_s and h_u is the height above the sea level of the radiosonde base and the upper limit of the water vapour occurrence, respectively. In [3] it is supposed to stop the integration at the air pressure level of 300 hPa.

In Fig. 3 you can see the course of the integrated water vapour content per average month for given exceedance probabilities (50,20,10,...,0.5%) being parameters of curves. 100% time corresponds to each month and time of soundings.

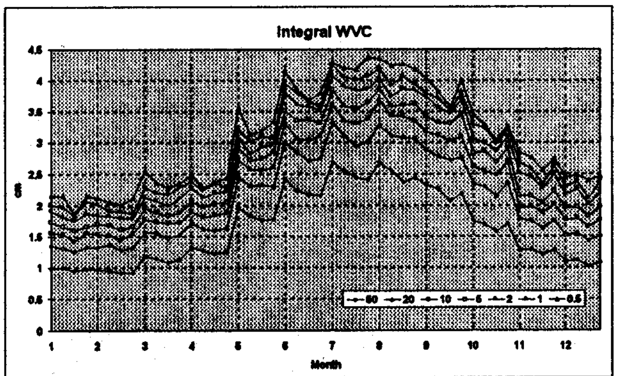

Fig.3: Integral Water Vapour Content [cm] (=10[kg.m^{-2}], which is exceeded at X% of 6hour periods considered. Values of X are shown in the legenda.

From Fig.3 it can be deduced that the seasonal variation is greater that the diurnal one. The average diurnal changes of the water vapour (WV) attenuation do not exceed 12% The annual distribution of the water vapour attenuation in Fig.4 confirms this fact. The average seasonal attenuation changes are greater than 100%. The attenuation maximum is at 00.00 UTC but the attenuation at 18.00 UTC is comparable with the attenuation at 00.00 UTC in the period September - February. The attenuation at 12.00 UTC is the smallest one, generally speaking. The seasonal maximum is in July and August, in the period from November to February there is a minimum of vapour attenuation from the seasonal point of view.

Fig.5 shows the WV attenuation for the worst month ("worst" value from each month was selected at given probability level). It can be again deduced that the diurnal variation is not very significant.

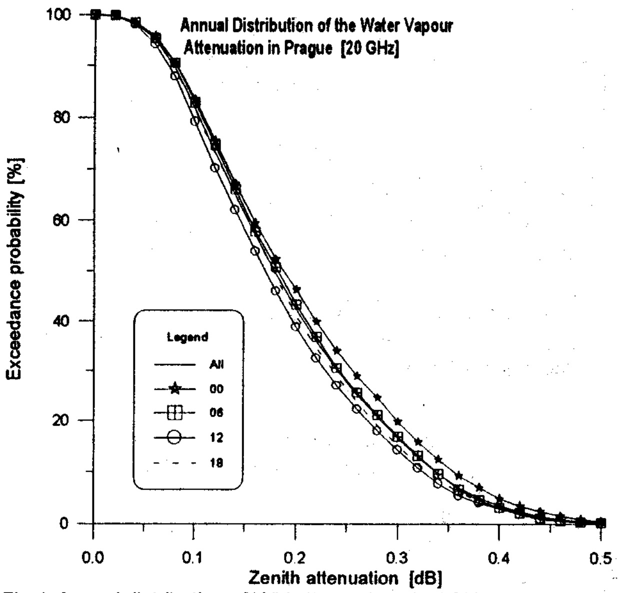

Fig.4: Annual distribution of WV attenuation at 20GHz.

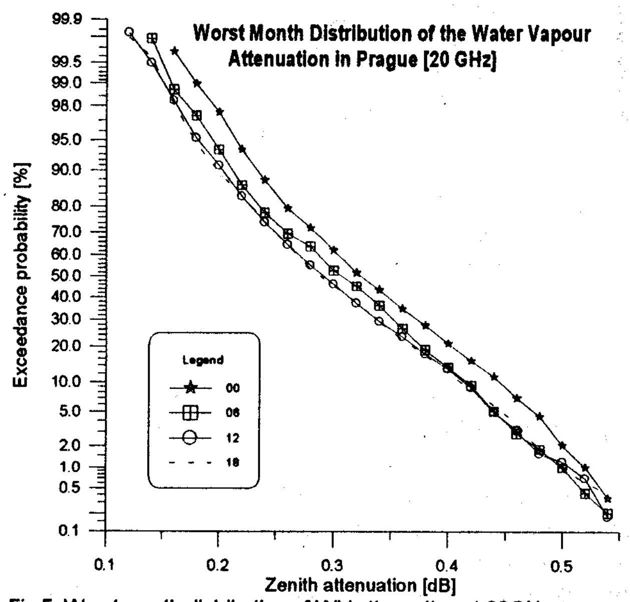

Fig.5: Worst month distribution of WV attenuation at 20GHz.

From the figures it seems that the integrated WVC distribution obeys the Normal (Gauss) distribution as it was supposed in literature at least in the summer period. Next table shows the *WVC* [cm] on the 1% exceedance probability level. The table also shows that the worst time per day is at 00 UTC.

Time	Annual	July	Worst m.
00 UTC	**387**	**420**	**420**
06 UTC	355	403	403
12 UTC	355	403	412
18 UTC	363	403	403
All	371	412	420

4. Cloud attenuation

4.1. Exact Technique

The specific cloud attenuation γ_c [dB/km] is usually computed by Liebes's method [4]:

$$\gamma_c = 0.819 f\, G(t,f) w \tag{4a}$$

where

$$G(t,f) = \frac{\varepsilon_i(t,f)}{\varepsilon_r^2(t,f) + \varepsilon_i^2(t,f) + 4 * [1 + \varepsilon_r(t,f)]} \tag{4b}$$

where ε is the complex permitivity of the cloud water, which depends on frequency and temperature (see [2] for formulas), *f* is the frequency [GHz] and *w* is the cloud water content [kg/m^3].

Cloud water content *w* [kg/m^3] occurs in clouds and it is responsible for the cloud attenuation of microwaves. Unfortunately it is not a directly measurable quantity. It can be estimated from temperature (empirical formula is shown in [2]).

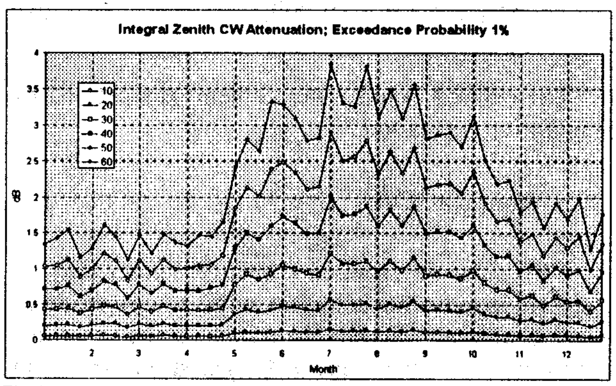

Fig.6a: Integral zenith Cloud Water Attenuation [dB], which is exceeded at 1% of 6hour periods considered. The frequency [GHz] is shown in the legenda.

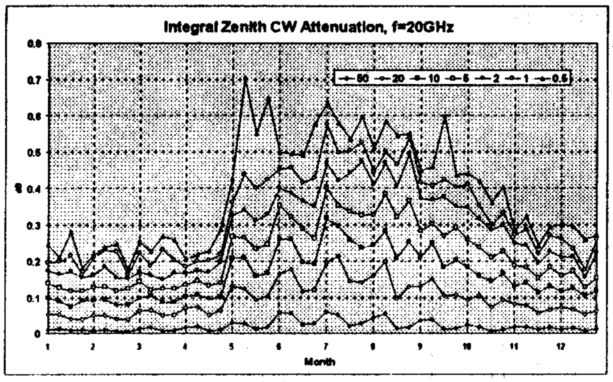

Fig.6b: Integral zenith Cloud Water Attenuation [dB] at the frequency 20 GHz, which is exceeded at X% of 6hour periods considered. Values of X are shown in the legenda.

The vertical integral of the specific cloud attenuation (between cloud base and cloud top) gives the zenith attenuation (see Annex to detect the cloud base and top). It is necessary to integrate not only the liquid water content w but also the product of the liquid water content and the auxiliary function $G(t,f)$ (temperature in a cloud is not constant). Therefore it is not possible to declare that the cloud attenuation is simply proportional to the integrated liquid water content as in the case of water vapour attenuation.

The seasonal and diurnal course of the cloud attenuation is shown in Fig. 6a (for 1% exceedance probability, frequency is a parameter) and in Fig. 6b (for 20 GHz, exceedance probability is a parameter).

4.2. Engineering Technique

The authors of [2] have proposed a simplified method to compute the cloud attenuation A_c based on the integrated reduced cloud water content CWC_{red}

$$A_c = 0.819 f G[f, 0^\circ C] * CWC_{red} \tag{5}$$

$$CWC_{red} = \int_{h_b}^{h_t} w_{red}(h_c)\,dh_c \tag{6}$$

The reduced liquid water content was defined by the following expression:

$$\gamma_c(f, w_{red}, 0^\circ C) = \gamma_c(f, w, t) \tag{7}$$

CWC_{red} for the required exceedance probability is published in radioclimatological maps. We have proved a good conformity between the results of the simplified method and the exact method based on the path integration of the specific cloud attenuation (at the frequencies 10-60GHz). Therefore, the study of diurnal and seasonal variation of the cloud attenuation can be reduced to the study of variation of CWC_{red}.

4.3. Diurnal and Seasonal Variations of the Integrated Reduced Cloud Water Content

Fig.7 shows the diurnal and seasonal variation of CWC_{red} for the given exceedance probabilities. We can see again the dominancy of seasonal (up to 300%) to diurnal (up to 35%) variation. The cloud attenuation dominates in the summer period (May-October), July seems to be the worst calendar month.

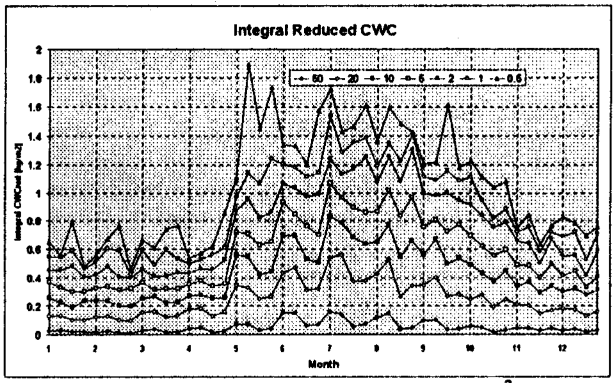

Fig.7: Integral reduced Cloud Water Content [kg/m^2], which is exceeded at X% of 6hour periods considered. Values of X are shown in the legenda.

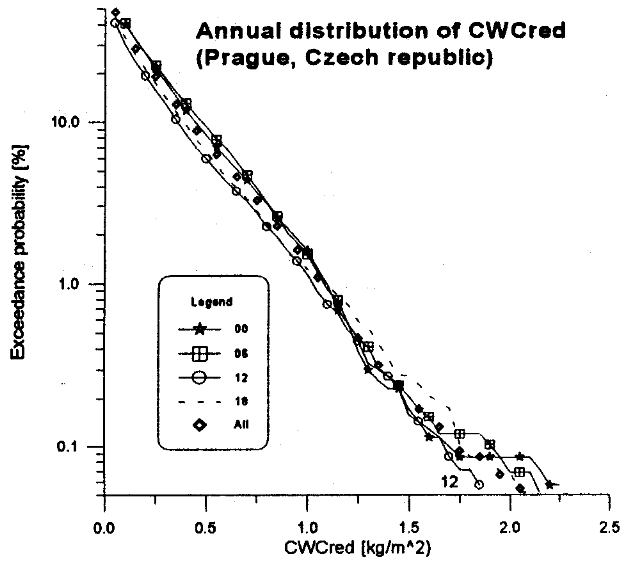

Fig.8: Annual distribution of CWC_{red} .

Fig.8 shows the annual distribution of CWC_{red} at four points of time per day. The worst month distribution of CWC_{red} is shown in Fig. 9. From these figures the exponential character of CWC_{red} distribution is obvious.

The next table compares the CWC_{red} values in [kg/m^2] on 1% exceedance probability level for average year (annual), average July and for the worst month. The maximum predominates at 18 UTC. The CWC diurnal variations exceed the WVC diurnal variations.

Time	Annual	July	Worst m.
00 UTC	0.95	**1.55**	**1.55**
06 UTC	0.90	1.30	1.40
12 UTC	1.03	1.35	1.35
18 UTC	**1.10**	1.40	**1.55**
All	1.05	1.35	1.55

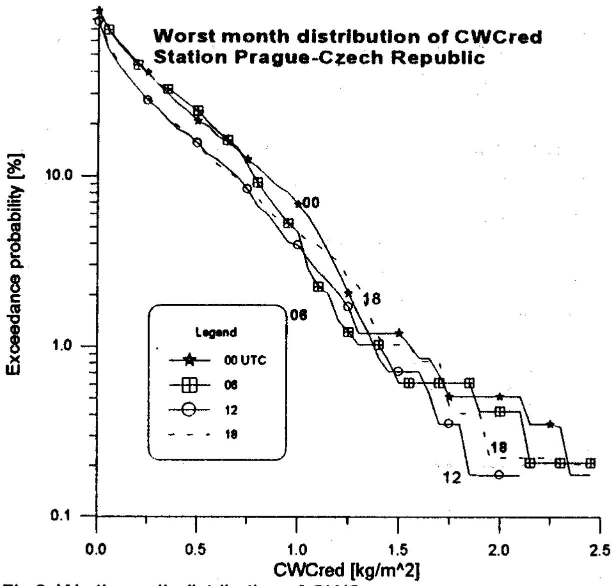

Fig.9: Worth month distribution of CWC_{red}.

The above analysis shows that the seasonal variation influences the attenuation much more than the daily variation in the water vapour as well as in the cloud attenuation case. The diurnal variations play a greater role in the summer period (May, June, July and September) in the WVC as well as in the CWC case. Generally speaking the diurnal minimum of the cloud and water attenuation can be expected at 12.00 UTC while the seasonal minimum of cloud and water vapour attenuation is reached between November and April.

5. ANNEX: Cloud detection

The presence of cloud was detected from sounding profiles in accordance with [2]. If the relative humidity is greater than the critical value U_c the cloud is present. The critical humidity U_c is given by the equation:

$$U_c = 1 - \alpha\sigma(1-\sigma)(1+\beta[\sigma - 0.5]) \quad [-] \qquad (8)$$

where $\alpha=1$, $\beta=\sqrt{3}$, and σ is ratio of the pressure on the considered level and at the surface level.

Acknowledgement: The activity was supported by the COST255 and by the Grant 205/96/1555 GA CR.

References

[1] Fišer O.: Prediction of Rain and Water Vapour Attenuation at Frequencies 10-30 GHz. Radioengineering, Vol.5, No.3, 1996.

[2] Salonen E., Uppala S.: New prediction method of Cloud Attenuation. Electronics Letters, Vol.27, No.12, 1991, pp.1106-1108.

[3] Salonen E., Karhu S., Uppala S., Hyvonen R.: Study of Improved Propagation Predictions. Final report for ESA under Estec contract 9455/91/NL/LC(SC), ESA, Contract report, December 1994.

[4] Liebe H.J.: MPM-An Atmospheric Millimeter - Wave Propagation Model. Int. J. of Infrared and Millimeter Waves, Vol.10, pp.631-650,1989.

About authors...

Ondřej FIŠER received Dipl. Ing. degree in electrical engineering (1977) and Ph.D. degree (1986) both from the Czech Technical University in Prague. He works as a scientific researcher at the Institute of Atmospheric Physics of the Czech Academy of Sciences. Professional interests: radiowave propagation in atmosphere, radar meteorology, radioclimatology, teaching. For more see http://www.ufa.cas.cz/html/meteo/fiser.html.

Daniela ŘEZÁČOVÁ graduated from Mathematical and Physical Faculty, Charles University Prague, in 1965. She received her RNDr. and CSc. degrees in 1972. She heads Meteorological Department of the Institute of Atmospheric Physics AS CR. Her research activity is focused on Mesoscale Meteorology, especially on Physics of Clouds and Precipitation.